# Synthesizing the impacts of baseflow contribution on C-Q relationships across Australia using a Bayesian Hierarchical Model

Danlu Guo[1], Camille Minaudo[2], Anna Lintern[3], Ulrike Bende-Michl[4], Shuci Liu[1], Kefeng Zhang[5], Clément Duvert[6,7]

5  [1] Department of Infrastructure Engineering, University of Melbourne, Victoria, 3010, Australia

[2] EPFL, Physics of Aquatic Systems Laboratory, Margaretha Kamprad Chair, Lausanne, Switzerland

[3] Department of Civil Engineering, Monash University, Victoria, 3800, Australia

[4] Bureau of Meteorology, 2601 Canberra, Australia

[5] Water Research Centre, School of Civil and Environmental Engineering, UNSW Sydney, High St, Kensington, NSW 2052,
10  Australia

[6] Research Institute for the Environment and Livelihoods, Charles Darwin University, Darwin, NT, Australia

[7] National Centre for Groundwater Research and Training (NCGRT), Australia

*Corresponding author's email address: anna.lintern@monash.edu

*Correspondence to*: Danlu Guo (danlu.guo@unimelb.edu.au)

**Abstract.** The spatial and temporal variation of concentration-discharge (C-Q) relationships inform solute and particulate export processes. Previous studies have shown that the extent to which baseflow contributes to streamflow can affect C-Q relationships in some catchments. However, these patterns have not yet been investigated across large spatial scales. To address
20   this, the study aims to assess how baseflow contributions, as defined by the median catchment baseflow index ($BFI\_m$), influence C-Q slopes across 157 catchments in Australia spanning five climate zones. This study focuses on six water quality variables: electrical conductivity (EC), total phosphorus (TP), soluble reactive phosphorus (SRP), total suspended solids (TSS), nitrate–nitrite (NOx) and total nitrogen (TN). The impact of baseflow contribution is explored with a novel Bayesian hierarchical model.

25   We found that $BFI\_m$ has a strong impact on C-Q slopes. C-Q slopes are largely positive for nutrient species (NOx, TN, SRP and TP) and are steeper in catchments with higher $BFI\_m$ across all climate zones (for TN, SRP and TP). On the other hand, we also found a generally higher variation in instantaneous BFI for catchments with high $BFI\_m$. Thus, the steeper C-Q slopes found in catchments with high $BFI\_m$ may be a result of a larger variation in water sources and flow pathways between low (baseflow-dominated) and high (quickflow-dominated) flow conditions. In contrast, catchments with low $BFI\_m$ may have
30   more homogeneous flow pathways at both low and high flows, resulting in less variable concentrations and thus a flatter C-Q slope. Our model can explain over half of the observed variability in concentration of TSS, EC and P species across all catchments (93% for EC, 63% for TP, 63% for SRP, and 60% for TSS), while being able to predict C-Q slopes across space by $BFI\_m$. This indicates that our parsimonious model has potential for predicting the C-Q slopes for catchments in different climate zones, and thus improving the predictive capacity for water quality across Australia.

## 1 Introduction

Understanding the causes of spatiotemporal variability in riverine chemistry is critical to support water quality management for both human and environmental end-uses. The relationship between the river chemistry and streamflow (concentration-discharge, or C-Q relationship) often shows distinct patterns that are specific to water quality variables and catchments. These are determined by (i) the spatial distribution of constituent sources within the catchment; and (ii) the interplay between the
40   biogeochemical and hydrological processes, which controls constituent mobilisation and transport through the catchment (Ebeling et al., 2021; Godsey et al., 2019; Musolff et al., 2015). The C-Q relationship therefore tells us about the key catchment processes controlling river water quality. As such, the C-Q relationship can help informing catchment management and mitigation strategies to improve catchment water quality (Dupas et al., 2019; Moatar et al., 2020).

However, it is challenging to identify the key catchment processes from analysing C-Q relationships, due to the high variability
45   in water quality across both space and time. First, water chemistry and streamflow characteristics can vary significantly across multiple spatial scales, from small headwater catchments (Dupas et al., 2021; Jensen et al., 2019; McGuire et al., 2014) to basin and continental scales (e.g., Dupas et al., 2019; Ebeling et al., 2021; Heiner M. et al. under review). Many previous

studies have assessed the spatial variations in C-Q relationships for nutrients, carbon and geogenic water quality variables, which identified land use and management, lithology, and topography as critical drivers for these spatial variations (e.g.,

50 Ebeling et al., 2021; Minaudo et al., 2019). Second, high-frequency water quality monitoring studies have shown high temporal variability in water chemistry (e.g., Kirchner et al., 2004; Rode et al., 2016). Besides variation in concentrations, recent high-frequency monitoring also highlighted the high variability of C-Q relationships over time and especially between runoff events; these temporal changes are driven by a series of mechanisms such as chemical build-up and flushing under varying flow magnitudes, and contrasting baseflow contributions during different stages of runoff events (Bende-Michl et al., 2013; Knapp

55 et al., 2020; Musolff A: et al.; Rusjan et al., 2008; Tunqui Neira et al., 2020).

In the existing studies that explore the variation of C-Q relationships, hydrological characteristics of catchments have been highlighted as a key influencing factor, as it defines the flow pathways and magnitudes that are critical to the transport processes (Tunqui Neira et al., 2020a, 2020b). Several studies have highlighted that, within a particular catchment, the C-Q relationship (and thus export behaviour) is dependent on whether streamflow is dominated by baseflow or quickflow (Gorski

60 & Zimmer, 2021; Knapp et al., 2020; Minaudo et al., 2019). However, there is little understanding of how the overall baseflow contribution of a catchment impacts the catchment's C-Q relationship, and thus the catchment's export regime. Further, most existing studies that explored the impact of baseflow contribution on C-Q relationships focused on catchments in temperate climates in Europe and North America (e.g., Gorski & Zimmer, 2021; Minaudo et al., 2019; Musolff et al., 2015). This leads to a limitation in transferring and systematically comparing findings to other climate zones and other parts of the world.

65 The current knowledge gap in understanding catchment export regimes for regions other than Europe and North America was partially addressed in Lintern et al. (in review) and Liu et al. (in preparation), which explored C-Q metrics over a range of climate zones in Australia. Both studies highlighted consistencies in C-Q patterns across contrasting climates for individual water quality variables and suggested that the inherent properties of each water quality variable determine its C-Q relationships. However, the role of different baseflow contributions on C-Q relationships has not yet been examined.

70 This study aims to assess the impact of catchment baseflow contribution on C-Q relationships of sediment, nutrients and salts across a large number of catchments within different climate zones in Australia. We hypothesise that catchments located in different climate zones would show very different ranges and distributions of baseflow contributions, leading to contrasted responses in terms of catchment export patterns, as represented by C-Q slopes. With this analysis we also hypothesise that the C-Q slopes in Australian catchments can be predicted across space by baseflow contribution. We test these hypotheses with a

75 Bayesian hierarchical modelling approach, which will i) add new understanding to the sources and export patterns of water quality variables; ii) improve the predictive capacity of water quality variables by better prediction of C-Q relationships over space.

## 2 Method

### 2.1 Data and study catchments

80 **2.1.1 Water quality and flow data**

This study relies on water quality and streamflow data collected across Australia by seven state agencies. These include: the Department of Land, Water and Planning (VIC DELWP, Victoria); WaterNSW (New South Wales); Department of Resources and Department of Environment and Science (QLD DNRME, Queensland); Department for Water and Environment (SA DEW, South Australia); Department of Water and Environmental Regulation (WA DER, Western Australia); Department of
85 Primary Industries, Parks, Water and Environment (TAS DPIPWE, Tasmania) and Department of Environment, Parks and Water Security (NT DEPWS, Northern Territory).

All available water quality data were obtained from all seven state agencies in late 2019 and collated into a single national-scale database (see more details in Lintern et al., in review). Quality control of the data was performed using quality codes, flags and detection limits provided by individual state agencies. The dataset consists of a mixture of grab samples and high-
90 frequency (continuously measured) water quality data; a daily average is taken if more than one water quality sample was collected for any day at any site. This study focuses on six water quality variables: total suspended solids (TSS), total phosphorus (TP), soluble reactive phosphorus (SRP), total nitrogen (TN), nitrate–nitrite (NOx) and electrical conductivity (EC). These six variables have been included because they are of key concern for Australian riverine water quality and are well monitored across Australia both spatially and temporally, as illustrated in Lintern et al. (in review).

95 For each monitoring site for the abovementioned six variables, we also obtained the corresponding available daily streamflow data. These daily streamflow data were obtained from the same seven state agencies as listed above. At each site, any missing or erroneous data were identified by quality code (as detailed in Table S1, Supplementary Materials) and removed for subsequent analyses. The daily streamflow data generally had good quality, with a < 5% median percentage of missing or erroneous data for individual water quality variables (Table S2, Supplementary Materials). These gaps and low-quality samples
100 in the daily streamflow records were then filled in using streamflow modelled by the Australian Bureau of Meteorology (BoM)'s operational landscape water balance model (AWRA-L), which simulates daily streamflow across Australia (Frost et al., 2016).

For this study, we focused only on monitoring sites (catchments) with water quality and flow data that satisfy the following criteria:

105     1)   Having over 50 pairs of corresponding concentration and flow data points; this is to ensure that the C-Q relationships observed are unaffected by outliers (Lintern et al., in review).

    2)   Having water quality time-series that spans at least 3 years; this ensures that a wide range of water quality and flow conditions are captured (e.g., across different seasons, high and low flows).

3) At least 75% of the range of flow quantiles (with unconstrained bounds e.g., 5 to 80%, 10 to 85%) is covered by water
   quality samples; this ensures that C-Q relationships are not biased by samples obtained at high or low flows for
   individual catchments.

We found a total of 157 sites (catchments) that met the above criteria across all the six water quality variables. As the monitored
water quality variables vary between catchments, there were 50-83 catchments used to investigate each variable. These
catchments are distributed across five main Australian climate zones as defined by Lintern et al. (in review): arid,
Mediterranean, temperate, subtropical and tropical (Figure 1). A summary of the temporal coverage of water quality and flow
data is provided in Figure S1 in the Supplementary Materials. Water quality data generally cover the full range of flow quantiles
of individual catchments (Figure S2, Supplementary Materials). Some sites are biased towards high flows, which is likely due
to i) monitoring priority for high flow events to better represent export loads; ii) practical constraints to sample low flows in
intermittent rivers and ephemeral streams.
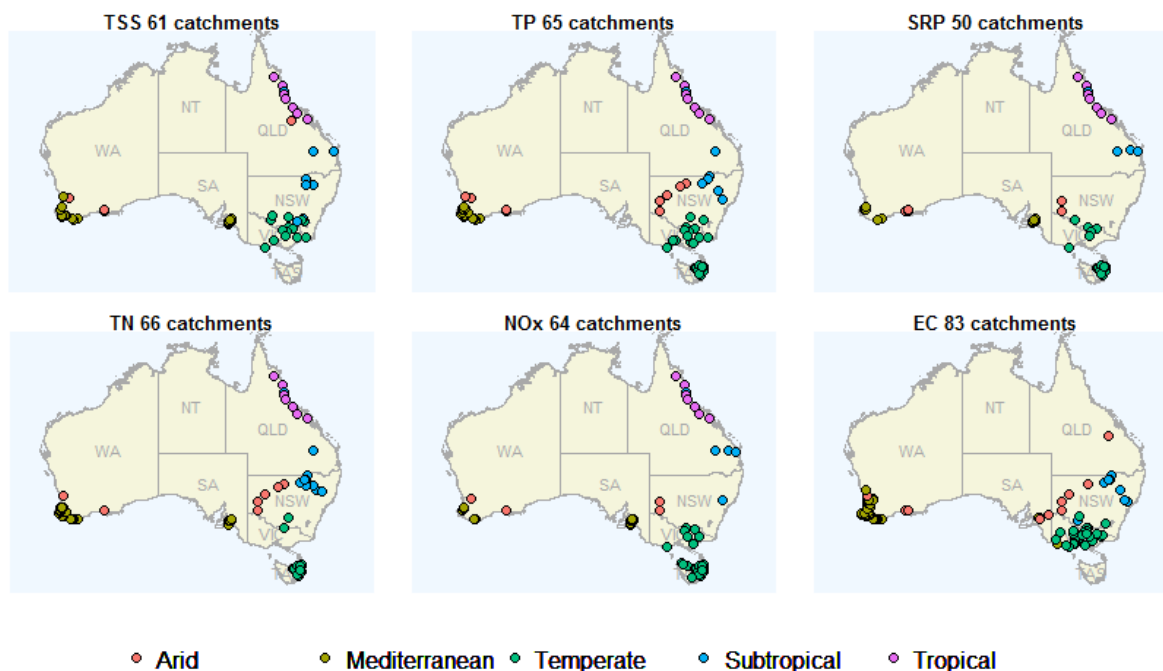
**Figure 1. Catchments included in study for each water quality variable (total number of catchments shown in panel titles). The colours denote five key climate zones in Australia. States and territories of Australia on the map are: New South Wales - NSW, Queensland - QLD, South Australia - SA, Tasmania - TAS, Victoria -VIC, Western Australia -WA, and Northern Territory - NT.**

**2.1.2 Representing catchment baseflow contribution with baseflow index**

To represent the overall contribution of baseflow to total streamflow in each catchment and explore how this impacts the C-Q
relationships across space, we used catchment baseflow index (BFI). BFI represents the proportion of discharge that occurs as

baseflow (Eckhardt, 2008; Lyne & Hollick, 1979; Nathan & McMahon, 1990; Zhang et al., 2017). We computed the catchment median BFI, *BFI_m*, based on daily BFIs derived from all flow records for each of the 157 catchments. The daily BFIs were estimated using a Lynne-Hollick baseflow filter with Alpha = 0.98 and a burn-in period of 30 days at both ends of the time

130 series, as recommended for Murray-Darling Basin in the south-eastern Australia (Ladson et al., 2013), within which a large number of the study catchments are located. We expect that the *BFI_m* can represent the typical flow regime at a catchment-level and differentiate between catchments with higher and lower baseflow contributions. In this way, we expect catchments with contrasting *BFI_m* to be dominated differently by surface flow and groundwater sources of water chemistry. Besides, *BFI_m*, we also computed the 10$^{th}$ and 90$^{th}$ percentiles of daily BFIs (*BFI_l*, *BFI_h*, respectively) for individual catchments to

135 explore how the distribution of BFI of each catchment can affect C-Q relationships.

### 2.2 Modelling the impacts of catchment baseflow contribution on concentration

We developed a Bayesian hierarchical model (BHM) to explore the effect of catchment BFI on C-Q slope. The BHM is advantageous in its 'borrowing power' across space (Gelman et al., 2013; Webb & King, 2009), which is highly effective to explain variability in spatial-temporal data under data-limited situations. Bayesian modelling is also effective for incorporating

140 uncertainty, which is necessary when analysing water quality data, as they are often associated with high uncertainty due to incomplete sampling of its natural variability (Guo et al., 2020; Liu et al., 2021).

The model considered a classic C-Q relationship for any site *s* at any time-step *t* (Eqn. 1), *where $\beta_s$ specifies the C-Q slope for a catchment* (Godsey et al., 2009):

$$\log(C_{s,t}) = \alpha_s + \beta_s \log(Q_{s,t}) \tag{1}$$

145 Our model used a modified version of Eqn. 1 based on previous literature on the effects of baseflow contribution on C-Q slopes within individual catchments (Gorski & Zimmer, 2021; Minaudo et al., 2019). We assume that for each water quality variable, the C-Q slopes of all catchments are following a normal distribution with a 'grand mean', *$\beta_0$*. Then the variation of C-Q slopes between catchments, away from *$\beta_0$*, are explained by changes in catchment BFI. The use of a mean C-Q slope is based on our preceding study, which suggested that for each water quality variable, export patterns (as represented by C-Q slopes) did not

150 differ between climate zones (Lintern et al., in review). The model conceptualization is illustrated in Figure 2 with observed flow time series from two catchments and calculated baseflow (panel a) and median BFI (*BFI_m*) (panel b); panel c) illustrates the modelled catchment C-Q slope with *BFI_m* considered as the main predictor. Two alternative model versions were also developed to incorporate the impacts of *BFI_l* and *BFI_h* in the same way.
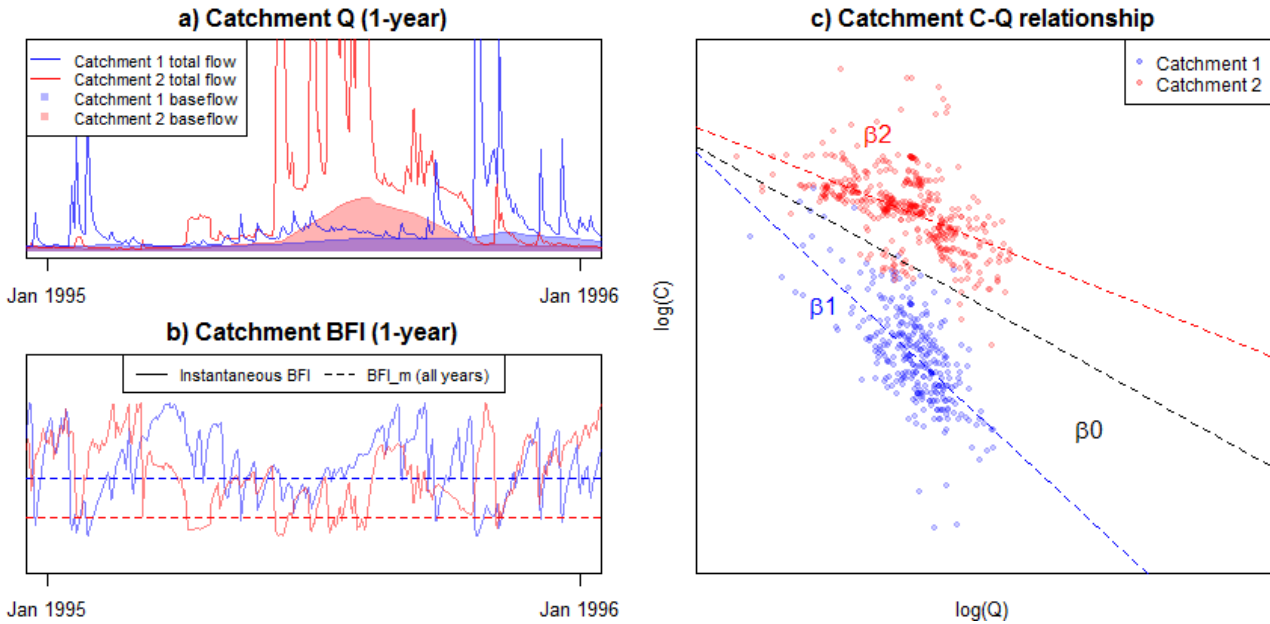
**Figure 2. Illustration of conceptualization of the BFI-based C-Q models with two catchments, with the catchment median BFI (*BFI_m*) as the main predictor of C-Q slope. a) flow time-series with shaded regions showing the baseflow contribution; b) BFI time-series and the corresponding *BFI_m*; and c) catchment C-Q relationships, in which the shift of C-Q slope of each catchment ($\beta_1$, $\beta_2$) away from the grand mean $\beta_0$ is determined by *BFI_m*. Both time-series for the instantaneous flow and BFI (a) and b)) are only shown for one year for visualisation.**

Thus, the resultant catchment C-Q slope $\beta_s$ is:

$$\beta_s = \beta_0 + BFI\_m_s \times \delta BFI_{climate} \qquad (2)$$

In Eqn. 2, the model parameter, $\delta BFI_{climate}$, represents the effect of *BFI_m* on C-Q slope. This effect is considered as a climate-specific parameter to assess whether the catchment BFI effects differ between climate. Such conceptualization of the BFI effects would then lead to a modified C-Q relationship for each catchment as:

$$log\left(C_{s,t}\right) = \alpha_s + (\beta_0 + BFI\_m_s \times \delta BFI_{climate}) \times log\left(Q_{s,t}\right) \qquad (3)$$

Equation 3 is the final form of the Bayesian hierarchical model, which was calibrated for each water quality variable across all catchments simultaneously to assess the impact of catchment BFI on C-Q slopes. The effects of *BFI_l* and *BFI_h* were explored with the same model structure.

To calibrate the Bayesian model, we used the R package *rstan* (Stan Development Team, 2018). The package first sampled parameter values from the Bayesian prior distributions with Markov chain Monte Carlo, and then evaluated candidate models to derive the posterior parameter distributions. Each of the unknown model parameters, $\beta_0$, $\alpha_s$ and $\delta BFI_{climate}$, was independently derived by sampling from a minimally informative normal prior distribution of *N(0,10)* (Gelman et al., 2013; Stan Development Team, 2018). We used four independent Markov chains in each model run, with a total of 50,000 model iterations

for each chain. Convergence of the chains was ensured by checking the *Rhat* value (Sturtz et al., 2005), which is a *rstan* output

175    that summarizes the consistency of the four Markov chains used in model calibration. Specifically, we ensured that the *Rhat* value is below 1.1, which suggested that the independent Markov chains have been well mixed and converged (Stan Development Team, 2018).

The calibrated model interpretation focused on the performance and the model parameter *δBFIclimate,* which informed the climate-specific effects of catchment BFI on C-Q slopes. We specifically assessed the following model outputs (results

180    presented in Section 3.3):

1)  *Model performance:* We assessed how well each BFI-based model (Eqn. 3) reproduced observed water quality with the Nash Sutcliffe Efficiency (NSE) (Nash & Sutcliffe, 1970). The NSE represents the proportion of observed variability that is explained by the model. As a benchmark, we also assessed the NSE of a baseline model which uses the classic C-Q relationship (Eqn. 1) observed for individual catchments to predict all water quality concentrations.

185    This baseline model represents the best performance that can be achieved to predict concentration using the catchment C-Q slopes together with flow. Therefore, the baseline model provides an informative benchmark to assess the BFI-based model.

2)  *Modelled effects:* We extracted the direction, magnitude and significance of the effects of catchment BFI from the posterior distribution of the calibrated model parameter, $\delta BFI_{climate}$, to assess the impact of catchment BFI on C-Q

190    slope for each climate zone.

## 3 Results and Discussions

In this section, we first discuss the spatial variation in the median BFI across the study catchments (Section 3.1). We then provide some examples at specific catchments to illustrate how catchment BFI can affect C-Q relationship as a proof of concept (Section 3.2). Section 3.3 then presents the inferences made with the BFI-based C-Q model, focusing on the model performance

195    in predicting water quality (Section 3.3.1), and we discuss the modelled effects of catchment BFI on C-Q slopes (Section 3.3.2). Note we focus on the outputs from the model which used the catchment median BFI (*BFI_m*) as the main predictor; the models calibrated using *BFI_l* and *BFI_h* as predictors generally show consistent performance and results with that of *BFI_m,* and are presented in the Supplementary Materials.

## 3.1 BFI across catchments

200    The range of catchment low, median and high BFIs (*BFI_l, BFI_m* and *BFI_h*) for all catchments included in this study are summarized in Figure 3. The calculated BFIs are consistent with previous studies of BFI patterns in Australian catchments (Zhang et al., 2017) and do not seem to correlate with catchment area (Figure S3, Supplementary Material). Generally, temperate catchments have the highest *BFI_m* across all climates, while similar ranges of median BFIs are seen between the

other four climate zones (Figure 3 a)). The *BFI_l* and *BFI_h* have consistent distributions with the median BFI across climate

205 zones. Considering the different catchments analysed between water quality variables, similar catchment BFI summaries were

also generated for each water quality variable, and the BFI distributions are generally consistent across different variables

(Figure S4, Supplementary Materials).
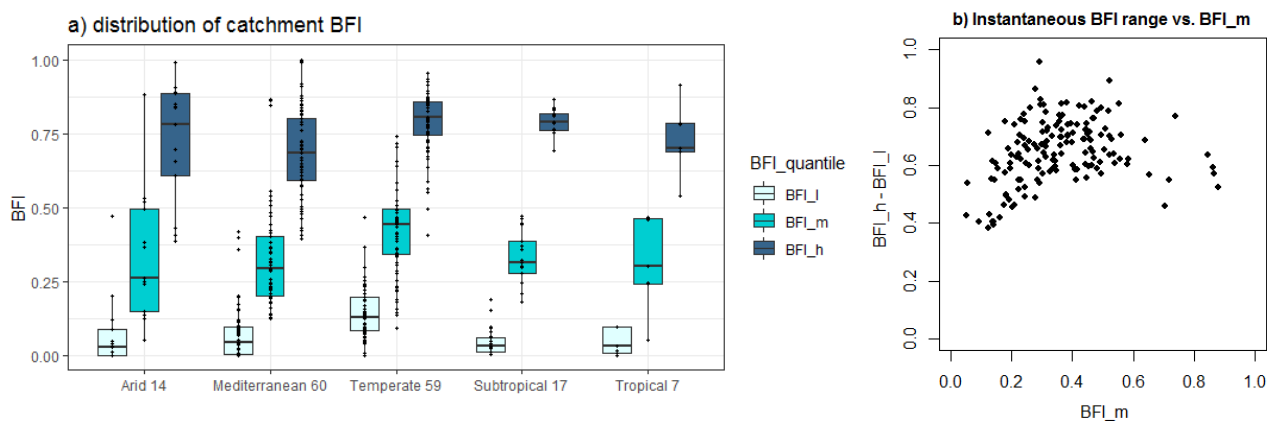
**Figure 3. a) Distribution of catchment low, median and high BFI (*BFI_l, BFI_m, BFI_h*) for each climate zone; b) range of**
210 **instantaneous BFI (*BFI_h – BFI_l*) versus *BFI_m*. Both plots include all 157 catchments across six water quality variables studied.**
**The corresponding versions of a) and b) for individual water quality variables are in Figure S4 and Figures S5 and S6**
**(Supplementary Materials).**

It is also worth noting that catchments with high *BFI_m* are likely to have a higher variability of instantaneous BFI, as

highlighted by the generally increasing differences between *BFI_h* and *BFI_l* with higher *BFI_m* (Figure 3 b)). The link

215 between *BFI_m* and variability of instantaneous BFI suggests potentially different flow pathways for catchments with

contrasting *BFI_m*. Specifically, a catchment with a low *BFI_m* tends to be associated with low instantaneous BFIs limited to

a small range; thus, the catchment is likely to always have lower contributions of baseflow and higher contributions of surface

flow, during both dry and wet conditions. In contrast, a catchment with a high *BFI_m* generally has a large range in

instantaneous BFIs. This means that the catchment is more likely switching between groundwater contributions in dry

220 conditions (high instantaneous BFI) and surface water contributions during wet conditions (low instantaneous BFI). Therefore,

catchments with higher *BFI_m* are more likely dominated by different flow pathways under dry and wet conditions.

### 3.2 Impact of BFI on C-Q slope: proof of concept

Before presenting the modelled effects of catchment baseflow contribution on C-Q relationships, we show some examples of

individual catchments to illustrate how C-Q relationships vary across catchments with *BFI_m*. We focus on the C-Q

225 relationships of TSS for four catchments including two arid catchments (ARIDa, ARIDb) and two tropical catchments (TROPa,

TROPb) (Figure 4). For each climate zone, we include one catchment with low *BFI_m* (ARIDa, TROPa) and another one with

high *BFI_m* (ARIDb, TROPb), relative to the corresponding range of *BFI_m* for TSS (Figure S4).
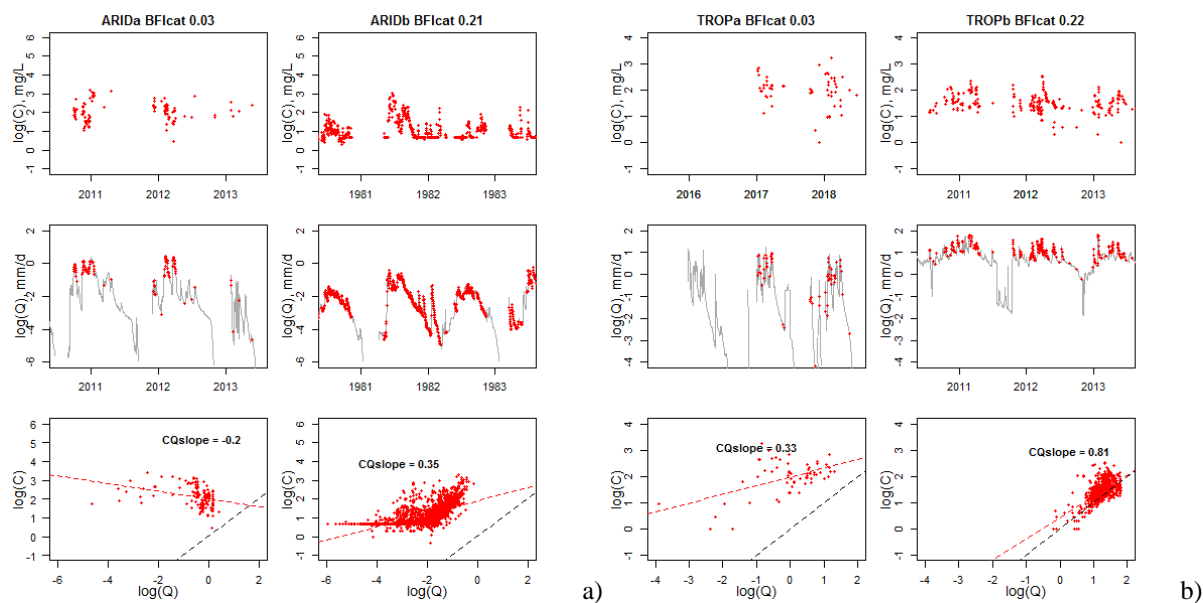
**Figure 4. C-Q relationships between TSS and flow for four individual catchments (in columns), including: a) two arid catchments (ARIDa, ARIDb); and b) two tropical catchments (TROPa, TROPb). Within each climate, a low-BFI and a high-BFI catchments are included, with the corresponding *BFI_m* shown in column titles. The top and middle rows for each catchment show a 3-year timeseries for the records of TSS concentrations and the continuous records of flow, with red dots showing the timesteps of water quality samples. The bottom row shows the C-Q relationship with all concentration and flow data at each catchment; the red dashed lines show the observed C-Q slope and the black dashed lines show the reference 1:1 line. All values plotted are in log-10 scale.**

Due to the particulate nature of TSS, we would expect the C-Q relationship to show strong a mobilisation behaviour that is enhanced during events (Musolff et al., 2015). Thus, catchments should have positive C-Q slopes, with a greater slope at a catchment with low *BFI_m*. However, our results show this is not always the case (Figure 4). The low-BFI arid catchment (ARIDa, *BFI_m* = 0.03) has a negative C-Q slope, whereas the high-BFI catchment (ARIDb, *BFI_m* = 0.21) shows a non-linear C-Q relationship (in log-log space). The overall C-Q slope is positive, which however, consists of a negative slope for lower flows, followed by a positive slope when the flow passes a certain threshold. This is similar to the differences in C-Q slopes with high and low flows as seen in previous studies (e.g., Moatar et al., 2017), and suggests that the mobilisation behaviour for TSS is dependent on a threshold flow.

Both tropical catchments (TROPa and TROPb) exhibit positive C-Q slopes that are relatively linear (in log-log space), where seasonal pattern in TSS concentration are in phase with those of streamflow. This highlights consistently strong mobilisation behaviours, with a greater positive C-Q slope for the catchment that has a higher baseflow contribution (TROPb, *BFI_m* = 0.22). Overall, this preliminary analysis on a small subset of catchments suggests that BFI may indeed drive differences in C-Q relationships between catchments, and that these effects may vary across climate zones.

### 3.3 Modelled results from the BFI-based C-Q model

### 3.3.1 Model performance in predicting water quality

250   The calibrated BFI-based C-Q model, when using catchment median BFI (*BFI_m*) as the predictor, can generally explain 50%
of the observed variability for individual water quality variables (Table 1). For TP, TN, SRP and EC, the model can explain
54-93% of the observed variability; the explanatory power is lower for TSS and TN (NSE of 0.50 and 0.47, respectively).
Compared to the baseline model that predicts water quality with observed C-Q slopes for individual catchments (see details in
Section 2.2), the BFI-based model has only marginally lower performance with 0.01-0.04 decreases in NSE across all water
255   quality variables (Table 1, see Figures S7 and S10 in Supplementary Materials for corresponding plots of the model fit). This
suggests that the BFI-based model, while having the capacity to predict C-Q slope across space, can predict water quality
almost as well as using the observed C-Q slope. The good performance of the BFI-based model also suggests its suitability to
derive inferences of the impacts of catchment BFI on C-Q slopes. Using *BFI_l* and *BFI_h* instead of *BFI_m* as the predictor
only has minimal impacts on model performance (Table S3, Supplementary Materials).

260   **Table 1. Performance of the BFI-based model (with *BFI_m* as the main predictor) and the baseline model in predicting across all
catchments for individual water quality variables (in rows), summarized as Nash Sutcliffe efficiency (NSE). The corresponding plots
of the model fit are in Figures S7 and S10 in Supplementary Materials.**

| Water quality variable | BFI-based C-Q model | Baseline model |
|---|---|---|
| TSS | 0.50 | 0.53 |
| TP | 0.54 | 0.56 |
| SRP | 0.62 | 0.64 |
| TN | 0.47 | 0.50 |
| NOx | 0.54 | 0.58 |
| EC | 0.93 | 0.94 |

### 3.3.2 Modelled effects of BFI on C-Q slope across Australia

265   Our BFI-based C-Q model synthesized the patterns observed for individual catchments (as illustrated in Section 3.2) across
the Australian continent. The model suggests that catchment median BFI, *BFI_m*, has significant influence on the C-Q slope
for most climate zones and water quality variables, with some differences between climate zones. Figure 5 presents the median
and the 95th credible intervals of these modelled impacts for each water quality variable, derived from the Bayesian posterior
estimates of $\delta BFI_{climate}$ (Eqn. 3). The effect of catchment median BFI on C-Q slope is almost always significant, with the
270   95th credible intervals not crossing over 0 for most combinations of water quality variables and climate zones.
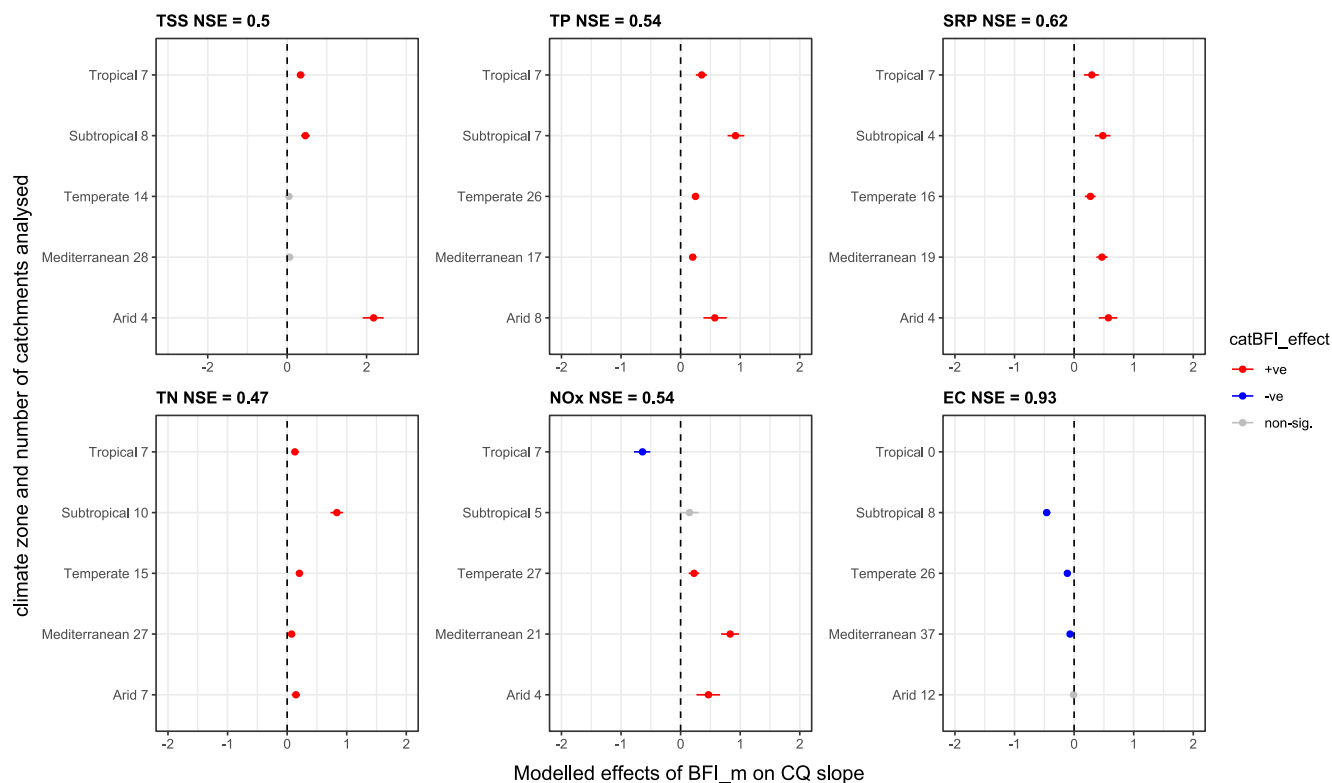
**Figure 5. Modelled effects of *BFI_m* on C-Q slope for each climate zone. The bars show the 95% credible interval (2.5th to 97.5th percentile) of modelled effect for each climate zone for each water quality variable, and the dots indicate the corresponding median levels. The colours indicate whether an effect is significantly positive, significantly negative, or non-significant; a positive effect means that C-Q slope increases with higher catchment BFI, and vice versa. Black dashed lines show zero-effect i.e. no effect at all.**

Figure 5 shows the directions of the impacts of catchment median BFI (*BFI_m*). To put the impacts of BFI into context, we show the modelled catchment C-Q slopes against the corresponding *BFI_m* values in Figure 6. Sediment and nutrients are largely dominated by mobilisation, as evidenced by the large proportion of positive C-Q slopes for TSS, TP, SRP, TN and NOx. In contrast, salts (EC) have largely negative C-Q slopes and are thus dominated by dilution. Regarding the effects of catchment BFI, we first note that for each water quality variable, the fitted relationships between C-Q slopes and BFI have a consistent 'diverging' pattern between climate zones. This is a result of our model structure, in which, for each water quality variable, all catchment C-Q slopes share a common 'grand mean' (Section 2.2), which represents the stable export patterns between climate zones as found in our preceding study (Lintern et al., in review). The deviation of slopes within each climate zone from the 'grand mean' is dependent on catchment *BFI_m* (Eqn. 2). Therefore, for catchments with low *BFI_m*, the differences in C-Q slopes between climate zones are smaller, and are all close to the 'grand mean'. Conversely, the C-Q slopes of catchments with high *BFI_m* are affected more strongly by the differences between climate zones.
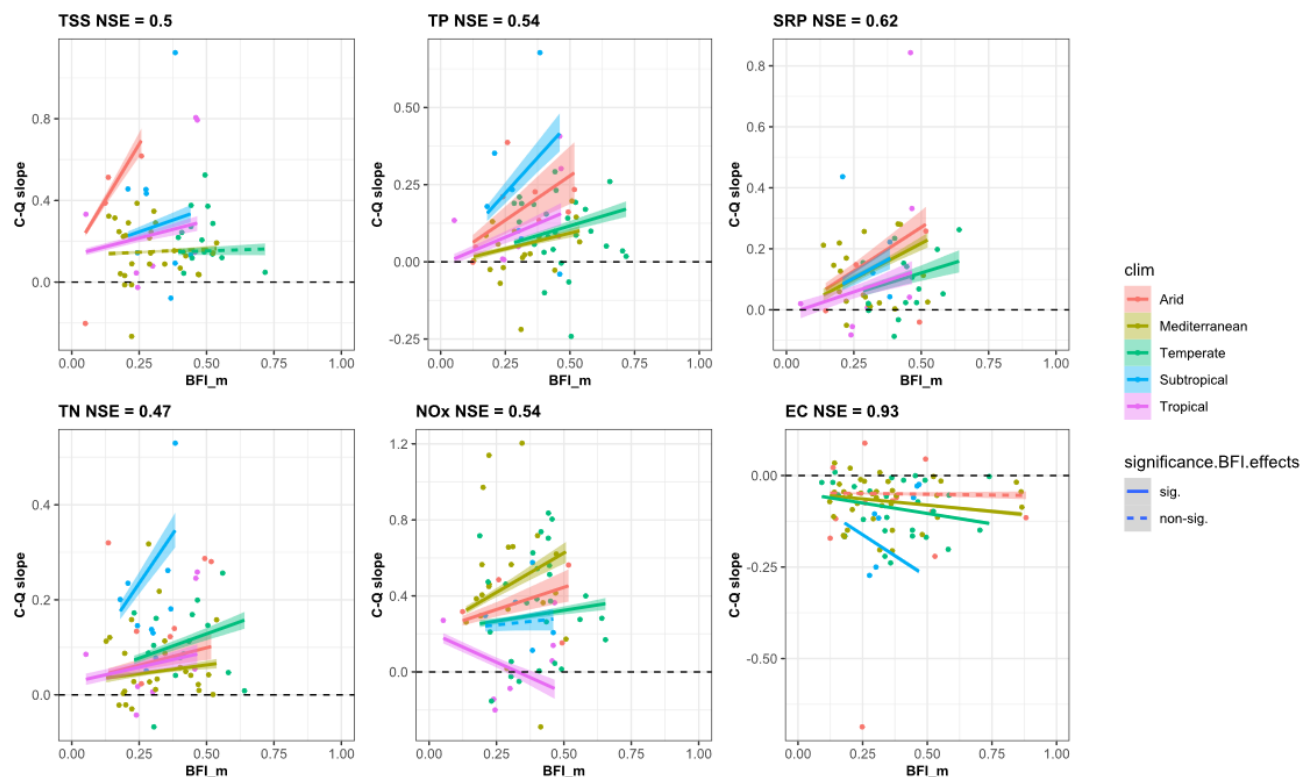
**Figure 6. Catchment C-Q slope vs. catchment median BFI (*BFI_m*), coloured by climate zones. The lines represent the modelled C-Q slope~*BFI_m* regression lines for individual climate zones, where *BFI_m* always has a significant impact on C-Q slope, based on the 95th credible intervals shown in Figure 5. The dots represent individual catchments. The black dashed lines mark a zero C-Q slope which differentiate mobilisation (C-Q slope>0) from dilution (C-Q slope<0).**

Across all six water quality variables and most climate zones, we found a general pattern that catchments with higher median BFI (*BFI_m*) tend to have steeper C-Q slopes (regardless of direction). This impact of *BFI_m* could be related to the negative correlation between *BFI_m* and the median concentrations combining with the low correlation between *BFI_m* and median flow (Figures S11 and S12, Supplementary Materials). The BFI effects are also unlikely related to longer travel times in larger catchments, as *BFI_m* is not correlated with catchment area (Figure S3). Considering export patterns, this result highlights an overall increase in i) mobilisation for sediment, nitrogen and phosphorus; and ii) dilution for salt, generally at catchments with higher baseflow contribution. In the subsequent discussions, we first detail the modelled effects for individual water quality variables, and then synthesise potential explanations related to catchment processes.

For both TP and SRP, across all climate zones, most catchments have positive C-Q slopes. This slope is steeper for catchments with higher *BFI_m* for all climates. To further interpret the behaviour of particulate and soluble P, we extracted the SRP:TP ratios for all catchments with both SRP and TP timeseries (Figure S13). The SRP:TP ratios for most catchments are less than 0.4, which suggests that TP is dominated by particulate forms across all catchments and climate zones. Combining this with

the positive effects of *BFI_m* seen for both SRP and TP, this suggests an overall mobilisation export pattern for both particulate

305    and soluble P, which is more pronounced at rivers with higher baseflow contributions.

For TN and NOx, the C-Q slopes are largely positive, and the modelling result suggests an increase in C-Q slope with *BFI_m* for most climate zones, except for subtropical (non-significant) and tropical (significantly negative) catchments for NOx. A large proportion of TN is present in particulate forms (Figure S14), with most catchments having NOx:TN ratios lower than 0.25. The particulate-dominated TN and the responses of its C-Q slope to *BFI_m* highlight that particulate N is largely

310    mobilised across all climate zones, which are enhanced with higher contributions of baseflow. For soluble N (NOx), the baseflow-driven mobilisation is also shown as an important pathway for arid, Mediterranean and temperate catchments.

For TSS, most catchments have positive C-Q slopes, which increase with *BFI_m* in arid, subtropical and tropical climates; the effects of *BFI_m* are non-significant for Mediterranean and temperate catchments. This 'enhancing' effect of *BFI_m* on positive C-Q slopes (i.e. mobilisation) is largely consistent with the results for TP and TN, which are both largely particulate-

315    bound.

EC exhibits mostly negative C-Q slopes, indicating an overall dilution export pattern. No tropical catchments were included due to insufficient data. A higher *BFI_m* led to a steeper negative C-Q slope for Mediterranean, subtropical and tropical catchments, but only has non-significant effect on C-Q slope for arid catchments. This result highlights stronger dilution behaviour at catchments with higher baseflow contribution, for Mediterranean, subtropical and tropical climates.

320    In summary, the above results highlight an overall greater absolute value of C-Q slope at a catchment with higher baseflow contribution. For sediment (TSS) and nutrients (N and P species), we see an overall mobilisation behaviour across Australian catchments, which is stronger in catchments with higher baseflow contribution. For salts (EC), we see an overall dilution behaviour, which is also enhanced at baseflow dominated catchments. The potential processes are discussed subsequently and summarized in Figure 7.
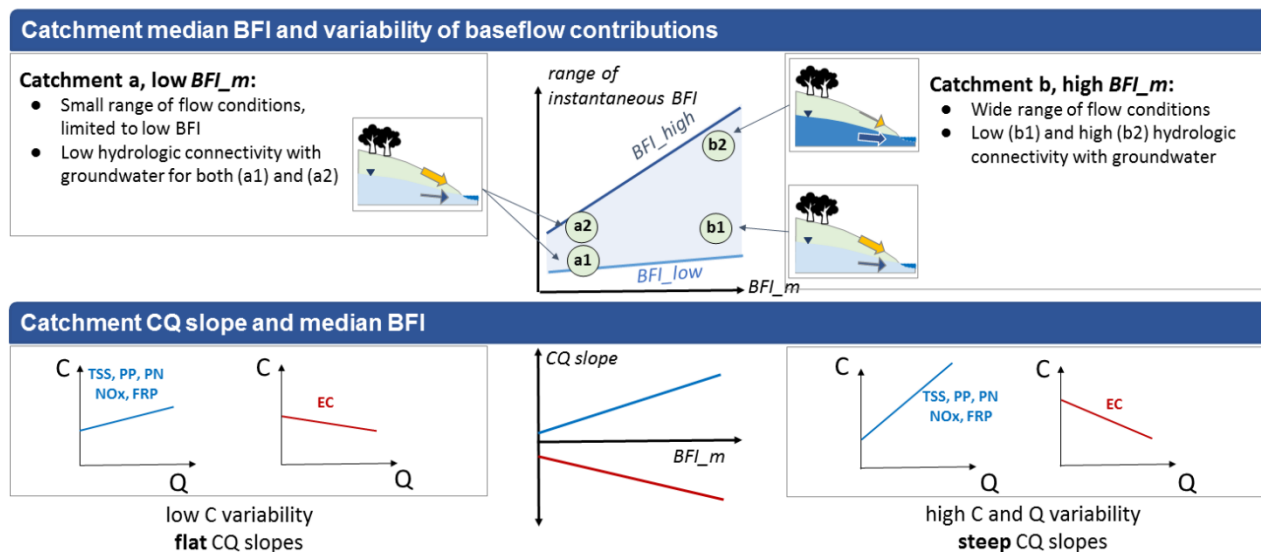
325

**Figure 7. Conceptual diagram of the modelled effect of baseflow contribution on C-Q slopes, for a catchment with low *BFI_m* (catchment a) and a catchment with high *BFI_m* (catchment b).**

For particulate water quality variables (TSS, and the largely particulate-bound part of TP and TN), our model result suggests that enhanced mobilisation in catchments with high *BFI_m*. This is a rather surprising result considering the dominance of

330  surface flow in transporting particulates (Lintern et al., 2018). One potential explanation relates to the higher variability of instantaneous BFI seen in catchments with high *BFI_m*, as seen in Figure 3b. Specifically, catchments with lower *BFI_m* generally have narrower ranges of instantaneous BFI, which thus tend to always have low baseflow contributions (i.e. surface flow dominated) regardless of dry or wet conditions (Catchment a, Figure 7). This can lead to a limited range of water sources with small variation of flow pathways to transport water chemistry to rivers, resulting in a relative stable export pattern across

335  low and high flows at these catchments. In contrast, catchments with higher *BFI_m* generally have higher variability in instantaneous BFI. This suggests higher variations in flow pathways, including surface flows dominance during wet period and subsurface flows dominance during dry period at these catchments (Catchment b, Figure 7). Consequently, these catchments can have a higher diversity of water sources and potentially larger gradients between groundwater-driven concentrations at low flow and runoff-driven concentrations at high flow.

340  For soluble N and P (NOx and SRP), our results also suggest enhanced mobilisation in catchments with high *BFI_m*. In Australian catchments, soluble N and P concentrations in the groundwater are generally low (Cartwright, 2020). This discards the case of rich nutrient inputs in groundwater due to the legacy of long-term agricultural practices, which is often observed in agricultural catchments in Europe and North America (Van Meter et al., 2017; Stackpoole et al., 2019; Ehrhardt et al., 2018). Thus, steeper C-Q slopes in Australian catchments with higher *BFI_m* could be interpreted as the result of a larger connectivity

345  between the stream and the vadose zone. However, as the case of TSS and particulate N and P, it is also plausible that the

enhanced mobilisation pattern seen in high *BFI_m* catchments rather results from the larger range of instantaneous BFI and thus more frequent mobilisation events. As discussed above, catchments with a greater variability in the instantaneous BFI are likely having greater gradients of concentrations for soluble N and P, between low groundwater-fed concentrations at low flow and high concentrations from surface/subsurface contributions at high flow. For the specific case of SRP, large oscillations of the groundwater table (which corresponds to large ranges of instantaneous BFI) were also shown to generate soil rewetting conditions favouring the release of soluble reactive P (Dupas et al., 2015; Gu et al. 2017).

The enhanced dilution export for EC (e.g. steeper negative C-Q slopes) in catchments with high *BFI_m* suggests the key role of deep flow pathways, which were found in catchments that have high groundwater concentrations of major ions (e.g., Zhi et al., 2019). The weaker effect of baseflow contribution for the arid and Mediterranean catchments can be the result of the overall less pronounced dilution patterns. Previous studies have found that in semi-arid areas, high evapotranspiration can lead to higher concentration of major ions in soil water or shallow groundwater compared with surface water, resulting in C-Q slopes close to 0 (e.g., Herczeg et al., 2001; Li et al., 2017).

Besides the abovementioned processes, another potential explanation for the modelled effects of *BFI_m* on C-Q relationships hypothesis is related to flow seasonality, which needs to be further explored. High baseflow contribution is generally found in more perennial catchments in Australia (Kennard et al., 2010), which might be associated with more clearly defined seasonal patterns in transporting water quality variables. These conditions are likely leading to well-defined C-Q relationships (Minaudo et al. 2019) and could result in steeper slopes compared to other catchments. In contrast, catchments with lower baseflow contribution are more likely driven by intermittent flow while lacking clear seasonal patterns, which leads to more scattered C-Q relationships. In this case, the absolute values of C-Q slopes tend to be close to 0 and these catchments often fall in the category of chemostatic with unclear export regimes (e.g. Godsey et al., 2009). However, we acknowledge that this hypothesis should be further tested, preferably with a subset of study catchments where high-frequency observations have been collected.

In summary, our results highlight the potential to improve understanding of transport processes via the relationships between water quality and baseflow contributions. Our model proved *BFI_m* useful in predicting C-Q slopes across space (Section 3.3.1), but also indicated that *BFI_m* may not be a suitable indicator to differentiate key flow pathways between catchments. Indeed, a high *BFI_m* may be associated with highly variable baseflow contributions involving both the surface and subsurface pathways, as illustrated in Figure 3 b). Therefore, a valuable avenue for future research would be to identify suitable BFI metrics to better represent the temporal dynamics of flow pathways to further improve the understanding of baseflow impacts on transport processes of water quality constituents.

## 4 Conclusions

In this study, a Bayesian hierarchical model was developed to understand the impacts of catchment baseflow contribution on C-Q slopes for six water quality parameters across Australia. These BFI-based models show good performances, which can

explain the majority of the observed variability in EC, SRP, TP, NOx and TSS (93, 62, 54, 54 and 50% explained, respectively) and almost half the observed variability for TN (47% explained). This highlights a potential parsimonious model that can be useful for predicting i) the C-Q slope across space; and ii) water quality for individual catchments, where flow data is available.

380 Our model suggests significant influences of catchment baseflow contributions - as represented by catchment median BFI - on C-Q slopes across most water quality variables and climate zones. One of the important findings is that the C-Q slopes are largely positive for both particular and soluble N and P (NOx, TN, SRP and TP), and are steeper for catchments with higher median BFI across all climate zones (for TN, SRP and TP). The enhanced mobilisation at catchments with higher median BFI is likely a result of more variable flow pathways, which introduces higher concentration gradients between low and high flows

385 that are dominated differently by groundwater and surface water sources. This result highlights the crucial role of flow pathways in determining catchment exports of water quality constituents, and the need of further studies to identify suitable baseflow metrics in differentiating flow pathways. The results also suggest a priority for managing and monitoring stream P and N, which should focus on catchments with the greater fluctuations in baseflow contributions.

This study complements our preceding study on the impacts of other catchment characteristics - including land use, land cover,
390 geology and climate - on C-Q slopes across Australia (Liu et al, in preparation). Further work should aim to synthesize the impacts of baseflow contribution and other spatial drivers by considering their interactions and establishing relative importance on influencing C-Q relationships.

This study also highlights the effectiveness of Bayesian hierarchical models in interpreting water quality data across large spatial scales. Such a model is ideal to analyse water quality data over a large number of catchments, with high heterogeneity
395 in temporal coverage and sampling frequency. This is particularly relevant for Australia, as water quality monitoring is often undertaken under different local/regional programs focusing on specific management interests.

**Data availability**

Water quality and flow data used this study are available upon request from seven Australian state agencies. These include: the Department of Land, Water and Planning (VIC DELWP, Victoria); WaterNSW (New South Wales); Department of
400 Resources and Department of Environment and Science (QLD DNRME, Queensland); Department for Water and Environment (SA DEW, South Australia); Department of Water and Environmental Regulation (WA DER, Western Australia); Department of Primary Industries, Parks, Water and Environment (TAS DPIPWE, Tasmania) and Department of Environment, Parks and Water Security (NT DEPWS, Northern Territory). Sources of data are detailed in Section 2.1.1.

**Author contribution**

405    All authors contributed to the design of the research. Danlu Guo carried out data collation, performed the simulations and prepared the manuscript with contributions from all co-authors. All authors contributed to the interpretation of the results and provided feedback.

**Competing interests**

The authors declare that they have no conflict of interest.

410    **Acknowledgement**

We would like to acknowledge that all water quality and flow data used in this study were accessed from the monitoring data collected by state agencies across Australia. In collecting these data, we were assisted by: Steve Tickell and Yuchun Chou (Department of Environment, Parks and Water Security, Northern Territory), Erinna Colton and Ashley Webb (WaterNSW, New South Wales), Christine Webb (The Department of Water and Environmental Regulation, Western Australia), David

415    Waters, Belinda Thomson, Ryan Turner, Rae Huggins (Department of Resources and Department of Environment and Science, Queensland), Bryce Graham (Department of Primary Industries, Parks, Water and Environment, Tasmania), Matt Gibbs (Department of for Water and Environment, South Australia), Paul Wilson (Department of Land, Water and Planning, Victoria). We also thank Professor Andrew Western, Ms Natalie Kho and Dr Rémi Dupas for their generous assistance in guiding this work and in data processing. Clément Duvert thanks Charles Darwin University for supporting a research visit to

420    the University of Melbourne in March 2020. We also acknowledge the Traditional Owners who were the first custodians of Australian waterways.

# References

Bende-Michl, U., Verburg, K., & Cresswell, H. P. (2013). High-frequency nutrient monitoring to infer seasonal patterns in catchment source availability, mobilisation and delivery. Environmental Monitoring and Assessment, 185(11), 9191-9219. doi:10.1007/s10661-013-324 Cartwright, I. (2020). Concentration vs. streamflow (C-Q) relationships of major ions in south-eastern Australian rivers: Sources and fluxes of inorganic ions and nutrients. Applied Geochemistry, 120, 104680. doi:https://doi.org/10.1016/j.apgeochem.2020.104680 6-8

Dupas, R., Gruau, G., Gu, S., Humbert, G., Jaffrézic, A., & Gascuel-Odoux, C. (2015). Groundwater control of biogeochemical processes causing phosphorus release from riparian wetlands. Water Research, 84, 307-314. doi:https://doi.org/10.1016/j.watres.2015.07.048

Dupas, R., Abbott, B. W., Minaudo, C., ,, & Fovet, O. (2019). Distribution of Landscape Units Within Catchments Influences Nutrient Export Dynamics. Frontiers in Environmental Science, 7(43). doi:10.3389/fenvs.2019.00043

Dupas, R., Causse, J., Jaffrezic, A., Aquilina, L., & Durand, P. (2021). Flowpath controls on high-spatial-resolution water-chemistry profiles in headwater streams. Hydrological Processes, 35(6), e14247. doi:https://doi.org/10.1002/hyp.14247

Dupas, R., Minaudo, C., & Abbott, B. W. (2019). Stability of spatial patterns in water chemistry across temperate ecoregions. Environmental Research Letters, 14(7), 074015. doi:10.1088/1748-9326/ab24f4

Ebeling, P., Kumar, R., Weber, M., Knoll, L., Fleckenstein, J. H., & Musolff, A. (2021). Archetypes and Controls of Riverine Nutrient Export Across German Catchments. Water Resources Research, 57(4), e2020WR028134. doi:https://doi.org/10.1029/2020WR028134

Eckhardt, K. (2008). A comparison of baseflow indices, which were calculated with seven different baseflow separation methods. Journal of Hydrology, 352(1), 168-173. doi:https://doi.org/10.1016/j.jhydrol.2008.01.005

Ehrhardt, S.; Kumar, R.; Fleckenstein, J. H.; Attinger, S.; Musolff, A. (2018). Decadal Trajectories of Nitrate Input and Output in Three Nested Catchments along a Land Use Gradient. Hydrol. Earth Syst. Sci. Discuss., 1–36. https://doi.org/10.5194/hess-2018-475.

Frost, A. J., Ramchurn, A., & Smith, A. (2016). The bureau's operational AWRA landscape (AWRA-L) Model. Retrieved from http://www.bom.gov.au/water/landscape/assets/static/publications/Frost__Model_Description_Report.pdf

Gelman, A., Carlin, J. B., Stern, H. S., Dunson, D. B., Vehtari, A., & Rubin, D. B. (2013). Bayesian Data Analysis, Third Edition: Taylor & Francis.

Godsey, S. E., Hartmann, J., & Kirchner, J. W. (2019). Catchment chemostasis revisited: Water quality responds differently to variations in weather and climate. Hydrological Processes, 33(24), 3056-3069. doi:https://doi.org/10.1002/hyp.13554

Godsey, S. E., Kirchner, J. W., & Clow, D. W. (2009). Concentration–discharge relationships reflect chemostatic
455    characteristics of US catchments. Hydrological Processes, 23(13), 1844-1864. doi:https://doi.org/10.1002/hyp.7315

Gorski, G., & Zimmer, M. A. (2021). Hydrologic regimes drive nitrate export behavior in human-impacted watersheds. Hydrol.
Earth Syst. Sci., 25(3), 1333-1345. doi:10.5194/hess-25-1333-2021

Gu, S.; Gruau, G.; Dupas, R.; Rumpel, C.; Crème, A.; Fovet, O.; Gascuel-Odoux, C.; Jeanneau, L.; Humbert, G.; Petitjean, P.
(2017). Release of Dissolved Phosphorus from Riparian Wetlands: Evidence for Complex Interactions among Hydroclimate
460    Variability, Topography and Soil Properties. Sci. Total Environ., 598, 421–431.
https://doi.org/10.1016/j.scitotenv.2017.04.028.

Guo, D., Lintern, A., Webb, J. A., Ryu, D., Bende-Michl, U., Liu, S. & Western, A. W. (2020). A data-based predictive model
for spatiotemporal variability in stream water quality. *Hydrology and Earth System Sciences*, 24(2), pp. 827-847.
doi:10.5194/hess-24-827-2020

465    Heiner M., Heaton M., Abbott B.W., White P., Minaudo C., & R., D. Model-based clustering of trends and cycles of nitrate
concentrations in Rivers across France. Submitted to Journal of the Royal Statistical Society.

Herczeg, A., Dogramaci, S., & Leaney, F. (2001). Origin of dissolved salts in a large, semi-arid groundwater system: Murray
Basin, Australia. Marine and Freshwater Research, 52(1), 41-52.

Jensen, C. K., McGuire, K. J., McLaughlin, D. L., & Scott, D. T. (2019). Quantifying spatiotemporal variation in headwater
470    stream length using flow intermittency sensors. Environmental Monitoring and Assessment, 191(4), 226. doi:10.1007/s10661-
019-7373-8

Kennard, M. J., Pusey, B. J., Olden, J. D., Mackay, S. J., Stein, J. L., & Marsh, N. (2010). Classification of natural flow regimes
in Australia to support environmental flow management. Freshwater Biology, 55(1), 171-193.
doi:https://doi.org/10.1111/j.1365-2427.2009.02307.x

475    Kirchner, J. W., Feng, X., Neal, C., & Robson, A. J. (2004). The fine structure of water-quality dynamics: the (high-frequency)
wave of the future. Hydrological Processes, 18(7), 1353-1359. doi:10.1002/hyp.5537

Knapp, J. L. A., von Freyberg, J., Studer, B., Kiewiet, L., & Kirchner, J. W. (2020). Concentration–discharge relationships
vary among hydrological events, reflecting differences in event characteristics. Hydrol. Earth Syst. Sci., 24(5), 2561-2576.
doi:10.5194/hess-24-2561-2020

480    Ladson, A. R., Brown, R., Neal, B., & Nathan, R. (2013). A standard approach to baseflow separation using the Lyne and
Hollick filter. Australasian Journal of Water Resources, 17(1), 25-34.

Li, L., Bao, C., Sullivan, P. L., Brantley, S., Shi, Y., & Duffy, C. (2017). Understanding watershed hydrogeochemistry: 2. Synchronized hydrological and geochemical processes drive stream chemostatic behavior. Water Resources Research, 53(3), 2346-2367. doi:https://doi.org/10.1002/2016WR018935

485 Lintern, A., Webb, J.A., Ryu, D., Liu, S., Bende-Michl, U., Waters, D., Leahy, P., Wilson, P., Western, A.W., (2018). Key factors influencing differences in stream water quality across space. Wires Water 51, e1260.

Lintern, A., Liu, S., Minaudo, C., Dupas, R., Guo, D., Zhang, K., Bende-Michl, U., Duvert, C. (in review). Climate controls on water chemistry states and dynamics in rivers across Australia. Submitted to *Hydrological Processes*

Liu, S., Ryu, D., Webb, J. A., Lintern, A., Guo, D., Waters, D. & Western, A. W. (2021). A Bayesian approach to understanding
490 the key factors influencing temporal variability in stream water quality - a case study in the Great Barrier Reef catchments. *Hydrology and Earth System Sciences*, 25(5), pp. 2663-2683. doi:10.5194/hess-25-2663-2021

Liu, S., Lintern, A., Minaudo, C., Dupas, R., Guo, D., Zhang, K., Bende-Michl, U., Duvert, C. (in preparation). Key factors affecting differences in spatial differences in water quality across Australian continent.

Lyne, V., & Hollick, M. (1979). Stochastic time-variable rainfall-runoff modelling. Paper presented at the Institute of
495 Engineers Australia National Conference.

McGuire, K. J., Torgersen, C. E., Likens, G. E., Buso, D. C., Lowe, W. H., & Bailey, S. W. (2014). Network analysis reveals multiscale controls on streamwater chemistry. Proceedings of the National Academy of Sciences, 111(19), 7030-7035. doi:10.1073/pnas.1404820111

Minaudo, C., Dupas, R., Gascuel-Odoux, C., Roubeix, V., Danis, P.-A., & Moatar, F. (2019). Seasonal and event-based
500 concentration-discharge relationships to identify catchment controls on nutrient export regimes. Advances in Water Resources, 131, 103379. doi:https://doi.org/10.1016/j.advwatres.2019.103379

Moatar, F., Abbott, B. W., Minaudo, C., Curie, F., & Pinay, G. (2017). Elemental properties, hydrology, and biology interact to shape concentration-discharge curves for carbon, nutrients, sediment, and major ions. Water Resources Research, 53(2), 1270-1287. doi:10.1002/2016wr019635

505 Moatar, F., Floury, M., Gold, A. J., Meybeck, M., Renard, B., Ferréol, M., et al. (2020). Stream Solutes and Particulates Export Regimes: A New Framework to Optimize Their Monitoring. Frontiers in Ecology and Evolution, 7(516). doi:10.3389/fevo.2019.00516

Musolff, A., Schmidt, C., Selle, B., & Fleckenstein, J. H. (2015). Catchment controls on solute export. Advances in Water Resources, 86, 133-146. doi:https://doi.org/10.1016/j.advwatres.2015.09.026

510 Musolff A:, Q. Zhan, R. Dupas, C. Minaudo, J. H. Fleckenstein, M. Rode, et al. Spatio-temporal Variability in Concentration-Discharge Relationships at the Event Scale. Under review in Water Resources Research.

Nash, J. E., & Sutcliffe, J. V. (1970). River flow forecasting through conceptual models part I — A discussion of principles. Journal of Hydrology, 10(3), 282-290. doi:https://doi.org/10.1016/0022-1694(70)90255-6

Nathan, R. J., & McMahon, T. A. (1990). Evaluation of automated techniques for base flow and recession analyses. Water Resources Research, 26(7), 1465-1473. doi:https://doi.org/10.1029/WR026i007p01465

Rode, M., Wade, A. J., Cohen, M. J., Hensley, R. T., Bowes, M. J., Kirchner, J. W., et al. (2016). Sensors in the Stream: The High-Frequency Wave of the Present. Environmental Science & Technology, 50(19), 10297-10307. doi:10.1021/acs.est.6b02155

Rusjan, S., Brilly, M., & Mikoš, M. (2008). Flushing of nitrate from a forested watershed: An insight into hydrological nitrate mobilization mechanisms through seasonal high-frequency stream nitrate dynamics. Journal of Hydrology, 354(1), 187-202. doi:https://doi.org/10.1016/j.jhydrol.2008.03.009

Stackpoole, S. M.; Stets, E. G.; Sprague, L. A. (2019). Variable Impacts of Contemporary versus Legacy Agricultural Phosphorus on US River Water Quality. Proc. Natl. Acad. Sci., 201903226. https://doi.org/10.1073/pnas.1903226116.

Stan Development Team. (2018). RStan: the R interface to Stan. R package version 2.18.1.

Sturtz, S., Ligges, U., & Gelman, A. E. (2005). R2WinBUGS: a package for running WinBUGS from R.

Tunqui Neira, J. M., Andréassian, V., Tallec, G., & Mouchel, J. M. (2020a). Technical note: A two-sided affine power scaling relationship to represent the concentration–discharge relationship. Hydrol. Earth Syst. Sci., 24(4), 1823-1830. doi:10.5194/hess-24-1823-2020

Tunqui Neira, J. M., Tallec, G., Andréassian, V., & Mouchel, J.-M. (2020b). A combined mixing model for high-frequency concentration–discharge relationships. Journal of Hydrology, 591, 125559. doi:https://doi.org/10.1016/j.jhydrol.2020.125559

Van Meter, K. J.; Basu, N. B.; Van Cappellen, P. (2017). Two Centuries of Nitrogen Dynamics: Legacy Sources and Sinks in the Mississippi and Susquehanna River Basins. Global Biogeochem. Cycles, 31 (1), 2–23. https://doi.org/10.1002/2016GB005498.

Webb, J. A., & King, L. E. (2009). A Bayesian hierarchical trend analysis finds strong evidence for large-scale temporal declines in stream ecological condition around Melbourne, Australia. Ecography, 32(2), 215-225. doi:doi:10.1111/j.1600-0587.2008.05686.x

Zhang, J., Zhang, Y., Song, J., & Cheng, L. (2017). Evaluating relative merits of four baseflow separation methods in Eastern Australia. Journal of Hydrology, 549, 252-263. doi:https://doi.org/10.1016/j.jhydrol.2017.04.004

Zhi, W., Li, L., Dong, W., Brown, W., Kaye, J., Steefel, C., et al. (2019). Distinct Source Water Chemistry Shapes Contrasting Concentration-Discharge Patterns. Water Resources Research, 55(5), 4233-4251. doi:https://doi.org/10.1029/2018WR024257